

Compressible magnetohydrodynamic turbulence in the Earth's magnetosheath: estimation of the energy cascade rate using *in situ* spacecraft data

L. Z. Hadid

*Swedish Institute of Space Physics, SE 751 21, Uppsala, Sweden and
LPP, CNRS, Ecole Polytechnique, Univ. UPMC, Univ. Paris-Sud,
Observatoire de Paris, Université Paris-Saclay, Sorbonne Université,
PSL Research University, 91128 Palaiseau, France*

F. Sahraoui

*LPP, CNRS, Ecole Polytechnique, Univ. UPMC, Univ. Paris-Sud,
Observatoire de Paris, Université Paris-Saclay, Sorbonne Université,
PSL Research University, 91128 Palaiseau, France*

S. Galtier

*LPP, CNRS, Ecole Polytechnique, Univ. UPMC, Univ. Paris-Sud,
Observatoire de Paris, Université Paris-Saclay, Sorbonne Université,
PSL Research University, 91128 Palaiseau, France and
Département de Physique, Université de Paris-Sud, Orsay, France*

S. Y. Huang

*School of Electronic Information, Wuhan University, Wuhan, China
(Dated: December 14, 2024)*

The first estimation of the energy cascade rate $|\epsilon_C|$ of magnetosheath turbulence is obtained using the CLUSTER and THEMIS spacecraft data and an exact law of compressible isothermal magnetohydrodynamics turbulence. $|\epsilon_C|$ is found to be of the order of $10^{-13} J.m^{-3}.s^{-1}$, at least three orders of magnitude larger than its value in the solar wind. Two types of turbulence are evidenced and shown to be dominated either by incompressible Alfvénic or magnetosonic-like fluctuations. Density fluctuations are shown to amplify the cascade rate and its spatial anisotropy in comparison with incompressible Alfvénic turbulence. Furthermore, for compressible magnetosonic fluctuations, large cascade rates are found to lie mostly near the linear kinetic instability of the mirror mode. New empirical power-laws are evidenced and relate $|\epsilon_C|$ to the turbulent Mach number and the internal energy. These new findings have potential applications in distant astrophysical plasmas that are not accessible to *in situ* measurements.

Turbulence is a ubiquitous non-linear phenomenon in hydrodynamic and plasmas flows that transfers dynamically energy between different scales. In astrophysical plasmas, turbulence is thought to play a major role in various processes such as accretion disks, star formation, acceleration of cosmic rays, solar corona and solar wind heating, and energy transport in planetary magnetospheres [1–4]. Thanks to the availability of *in situ* measurements recorded on board various orbiting spacecraft, the solar wind and the Earth's magnetosheath (i.e., the region of the solar wind downstream of the bow shock) provide a unique laboratory for the observational studies of plasma turbulence. An important feature of magnetosheath turbulence is the high level of density fluctuations in it, which can reach $\sim 50\% - 100\%$ [5–8] in comparison with $\sim 5\% - 20\%$ in the solar wind [9, 10]. This makes the magnetosheath a key region of the near-Earth space where significant progress can be made in understanding compressible plasma turbulence, which is poorly understood although it is thought to be important in various astrophysical plasmas, such as supernovae remnants or the interstellar medium (ISM) [11–15].

In the solar wind the magnetohydrodynamics (MHD) approximation has been successfully used to study turbulence cascade at scales larger than the ion inertial length (or Larmor radius) [16, 17]. As in neutral fluid turbulence, an inertial range of MHD turbulence is generally evidenced by the observation of a power spectral density (PSD) exhibiting a power-law over a wide range of scales. This power-law is a manifestation of a turbulent cascade of energy from large scales, where the energy is injected, to the smaller ones where the energy is dissipated. The energy transfer over scales is assumed to occur at a constant rate, which is equal to the rate at which energy is injected and dissipated into the system. This quantity carries therefore a major importance in modeling the processes of particle acceleration and heating in plasmas since it provides an estimation of the amount of energy that is eventually handed to the plasma particles at the dissipation scales [18]. Within the incompressible MHD turbulence theory, the energy cascade rate can be estimated using the so-called third-order law relating the longitudinal structure functions of the magnetic and the velocity fields, to the spatial scale l [19] (PP98

hereafter). The PP98 model has been used to estimate the cascade rate in the solar wind from the ACE and ULYSSES spacecraft data [20–26]. Those estimations were used to better understand the long-standing problem of the non-adiabatic heating of the solar wind observed at different heliospheric distances ($\sim 0.3 - 100$ AU, Astronomical Unit) by the Helios [27, 28], Pioneer and Voyager spacecraft [29–31]. To date no such estimation of the cascade rate exists for magnetosheath turbulence. The main reason for that being the complex nature of magnetosheath turbulence and the importance of density fluctuations in it, which requires going beyond the PP98 model to include compressibility. Recently, an exact law of compressible isothermal MHD turbulence has been derived [32] (hereafter BG13). It has been successfully used to improve our understanding of the role of density fluctuations in heating the fast and slow solar wind by showing in particular that, even if they are weak and represent only $\sim 5\% - 20\%$ of the total fluctuations, they nevertheless can enhance significantly the turbulence cascade rate [10, 33].

In the present Letter, we provide the first estimate of the energy cascade rate of compressible MHD turbulence in the Earth’s magnetosheath using the BG13 and *in situ* wave and plasma data. We investigate furthermore how density fluctuations amplify the energy cascade rate and how they affect its spatial anisotropy. The role of density fluctuations is highlighted by comparing the results obtained from the compressible BG13 and the incompressible PP98 exact laws. Under the assumptions of time stationarity, space homogeneity and isotropic turbulence, the PP98 exact law is given by

$$-\frac{4}{3}\varepsilon_I\ell = \left\langle \left(\frac{(\delta\mathbf{z}^+)^2}{2}\delta z_\ell^- + \frac{(\delta\mathbf{z}^-)^2}{2}\delta z_\ell^+ \right) \right\rangle \rho_0, \quad (1)$$

and the BG13 model is given by

$$\begin{aligned} -\frac{4}{3}\varepsilon_C\ell = & \left\langle \frac{1}{2} [\delta(\rho\mathbf{z}^-) \cdot \delta\mathbf{z}^-] \delta z_\ell^+ + \frac{1}{2} [\delta(\rho\mathbf{z}^+) \cdot \delta\mathbf{z}^+] \delta z_\ell^- \right\rangle \\ & + \langle 2\delta\rho\delta e\delta v_\ell \rangle \\ & + \left\langle 2\bar{\delta} \left[\left(1 + \frac{1}{\beta} \right) e + \frac{v_A^2}{2} \right] \delta(\rho_1 v_\ell) \right\rangle \end{aligned} \quad (2)$$

where $\mathbf{z}^\pm = \mathbf{v} \pm \mathbf{v}_A$ represent the Elsässer variables, \mathbf{v} being the plasma flow velocity, $\mathbf{v}_A \equiv \mathbf{B}/\sqrt{\mu_0\rho}$ is the Alfvén speed, $\rho = \rho_0 + \rho_1$ is the local plasma density ($\rho_0 = \langle \rho \rangle$ and ρ_1 are the mean and fluctuating density), $\delta\mathbf{z}^\pm \equiv \mathbf{z}^\pm(\mathbf{x} + \boldsymbol{\ell}) - \mathbf{z}^\pm(\mathbf{x})$ is the spatial increment of \mathbf{z}^\pm at a scale ℓ in the radial direction, $\langle \dots \rangle$ is the ensemble average, $\bar{\delta}\psi \equiv (\psi(\mathbf{x} + \boldsymbol{\ell}) + \psi(\mathbf{x}))/2$, $e = c_s^2 \ln(\rho/\rho_0)$ is the internal energy, with c_s the constant isothermal sound speed, and $\beta = 2c_s^2/v_A^2$ is the local ratio of the total thermal to magnetic pressure ($\beta = \beta_e + \beta_p$). Note that in the PP98 model, ρ is replaced by ρ_0 in the definition of the Alfvén speed. The reduced form of BG13

used here assumes furthermore the statistical stationarity of the plasma β and the negligible contribution of the energy source terms w.r.t. flux terms [33]. It is worth noting that contrary to incompressible MHD theory, the BG13 compressible model yields an energy cascade rate that is not simply related to third-order moments of the different fields increments but rather involves more complex combinations of the turbulent fields. In particular the last term in the RHS of equation 2, is written as a first order increment multiplied by an averaged quantity $\bar{\delta}\psi$.

Results — The data used here were measured by the CLUSTER and THEMIS B/C spacecraft in the terrestrial magnetosheath [34, 35]. Combining the data from the two missions was aimed only at increasing the number of analyzed events in our study for a better statistical convergence. The magnetic field measurements of CLUSTER come from the Flux Gate Magnetometer (FGM) [36], while the ion and electron plasma moments (density, velocity and temperature) come from the Cluster Ion Spectrometer (CIS) experiment [37], and the Plasma Electron and Current Experiment (PEACE) [38], respectively. A special attention has been paid to the reliability of the plasma data, in particular the plasma density measurements, through cross-checks between the PEACE, CIS and the WHISPER experiments [39] on board Cluster (we selected only intervals when the instruments were consistent with each other). For Themis spacecraft, the magnetic field data and the plasma moments are measured respectively by the FGM [40] and the ElectroStatic Analyzer (ESA) [41].

A large statistical survey of PSD of δB in the magnetosheath using the Cluster data showed that only a small fraction (17%) had a scaling close to the Kolmogorov spectrum $f^{-5/3}$ at the MHD scales, and were dominated either by incompressible Alfvénic or compressible magnetosonic fluctuations [42]. Those data sets correspond to a state of fully developed turbulence that is reached away from the bow shock toward the magnetosheath flanks. The remaining cases were found to have shallower spectra close to f^{-1} and were distributed essentially near the bow shock toward the nose of the magnetopause. *hadid et al.* [43] showed that the f^{-1} spectra were populated by uncorrelated fluctuations. Here, since we are interested in estimating the energy cascade rate, we focus only of the Kolmogorov-like cases that correspond to a fully developed turbulence where an inertial range can be evidenced. Considering only case studies characterized by the absence of velocity shears, our data selection resulted in 47 time intervals of equal duration 48 mn, which corresponds to a number of data points $N \sim 240$ in each interval with a 12 s time resolution ($N_{tot} \sim 2 \times 10^4$). The resulting samples were divided into two groups depending on the nature of the dominant turbulent fluctuations: incompressible Alfvénic-like and compressible magnetosonic-like ones. This was done

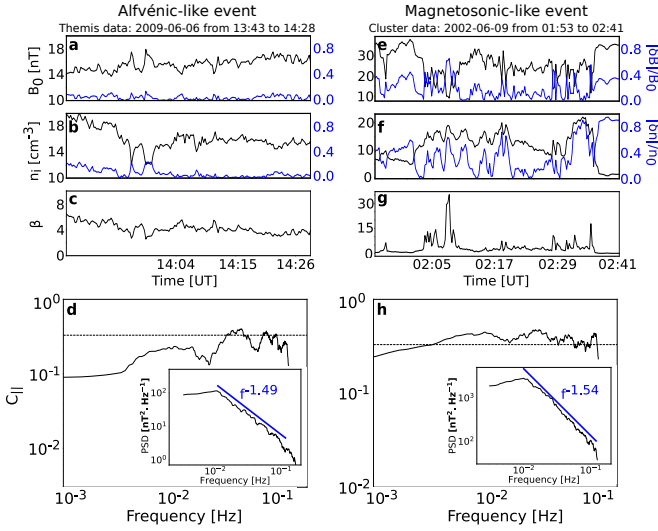


Figure 1: (a, e) The magnetic field modulus (black) and fluctuations (blue), (b, f) ion number density (black) and density fluctuations (blue) and (c, g) total plasma β . (d) and (h) the corresponding magnetic compressibility. The inset is the PSD of δB and the corresponding power-law fit in the inertial range (blue).

using the magnetic compressibility $C_{||} = \delta B_{||}^2 / \delta B^2$ (i.e., the ratio between the PSDs of the parallel to the total magnetic fluctuations; parallel being along the mean background field B_0) [43–46]. Figure 1 shows two examples of an Alfvénic-like event characterized by a nearly constant B , a subdominant $\delta B_{||}$ and weak density fluctuations, and a compressible case having large B and density fluctuations and a strong $\delta B_{||}$.

For each of these groups we computed the absolute values of the cascade rates $|\epsilon_C|$ and $|\epsilon_I|$ from the compressible BG13 and the incompressible model PP98, respectively. To do so, temporal structure functions of the different turbulent fields involved in equations 2 and 1 were constructed for different values of the time lag τ between 10s and 1000s in order to probe into the scales of the inertial range. It is worth noting that because of the low statistical samples we analyze, the change of sign of ϵ would give an unreliable estimate of the $\langle \epsilon_C \rangle$ and $\langle \epsilon_I \rangle$, the reason for which we considered only their absolute values and not the actual signed values. By applying a linear fit on the resulting energy cascade rates, we studied only the ones that are relatively linear with τ , **with no changes in the sign at least for one decade of scales..** Two main observations can be made from the two examples shown in Figure 2: first, the incompressible cascade rate $|\epsilon_I|$ is larger by a factor ~ 100 in the magnetosonic case compared to the Alfvénic one, which can be explained by the large amplitude δB in the former [10]. Second, density fluctuations in the magnetosonic case amplify $|\epsilon_C|$ by a factor ~ 7 w.r.t. $|\epsilon_I|$. The results of analysis of all the samples are summarized in

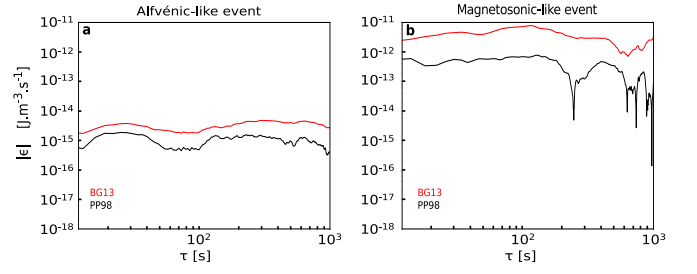


Figure 2: The energy cascade rates computed using BG13 (red) and PP98 (black) for the same (a) Alfvénic and (b) magnetosonic-like events of Figure 1.

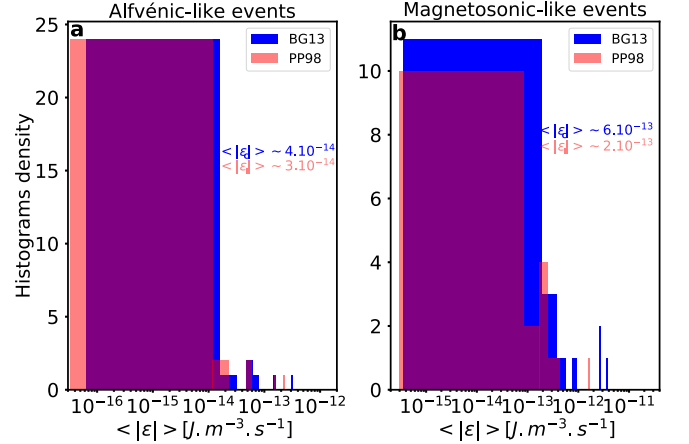


Figure 3: Histograms of $\langle |\epsilon_I| \rangle$ (red) and $\langle |\epsilon_C| \rangle$ (blue) computed using the exact laws of PP98 and BG13 for the (a) Alfvénic and (b) magnetosonic-like events.

Figure 3. As one can see in that figure, for the incompressible Alfvénic cases, the histograms of $\langle |\epsilon_C| \rangle$ (blue) and $\langle |\epsilon_I| \rangle$ (red), almost overlap and the mean values for both is of the order of $\sim 10^{-14} \text{ J} \cdot \text{m}^{-3} \cdot \text{s}^{-1}$, whereas for the compressible magnetosonic events the histogram of $\langle |\epsilon_C| \rangle$ (blue) is shifted towards larger values compared to $\langle |\epsilon_I| \rangle$ (red). The corresponding mean values are respectively $\sim 6 \times 10^{-13}$ and $\sim 2 \times 10^{-13} \text{ J} \cdot \text{m}^{-3} \cdot \text{s}^{-1}$.

Interestingly, the role of the compressibility in increasing the compressible cascade rate can be evidenced by the turbulent Mach number $\mathcal{M}_s = \sqrt{\langle \delta v \rangle^2 / c_s^2}$, where δv is the fluctuating flow velocity. Figure 4 shows a power law-like dependence of $\langle |\epsilon_C| \rangle$ on \mathcal{M}_s as $\langle |\epsilon_C| \rangle \sim \mathcal{M}_s^4$, steeper than the one observed in the solar wind [10]. To the best of our knowledge there are no theoretical predictions that relate ϵ to \mathcal{M}_s in compressible turbulence. However, in incompressible flows, dimensional analysis à la Kolmogorov yields a scaling that relates ϵ_I to the third power of \mathcal{M}_s . The high level of the density fluctuations in the magnetosheath seems to modify this scaling to the one we estimated here. Although more analytical and numerical studies are needed to understand the relationship between $|\epsilon_C|$ and \mathcal{M}_s , the scaling law obtained here

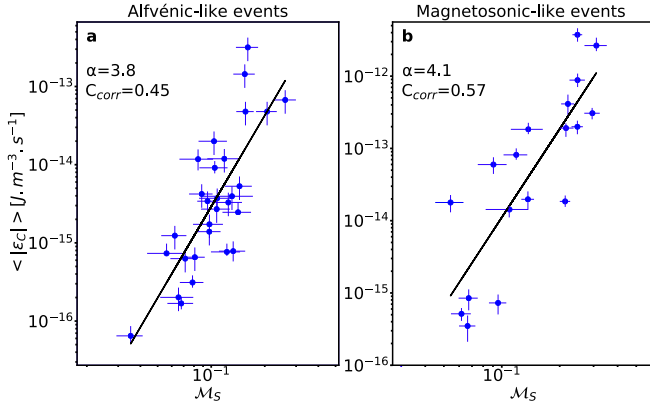


Figure 4: Compressible energy cascade rate as a function of the turbulent Mach number for the Alfvénic (a) and Magnetosonic-like (b) events. The black line represents a least square fit of the data, α is the slope of the power-law fit.

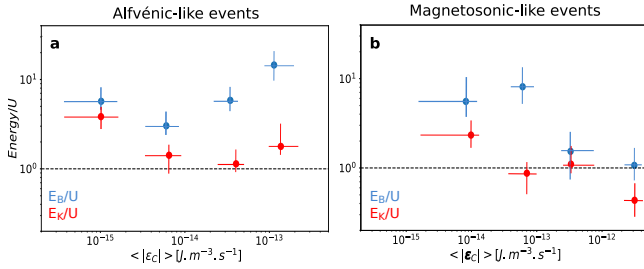


Figure 5: Normalized mean compressible magnetic (blue) and kinetic (red) energies to the internal energy as a function of the averaged compressible energy cascade rate for the Alfvénic (a) and magnetosonic (b) events.

may be used as an empirical model for other compressible media non accessible to *in-situ* measurements.

A good correlation is also evidenced between the leading order of compressible internal energy $U = \rho_0 c_s^2 \ln(1 + \rho_1/\rho_0)$ of the turbulent fluctuations and the cascade rate in the magnetosonic-like events. Figure 5 shows for each type of turbulent fluctuations the dependence of the normalized (to U) kinetic $E_K = \frac{1}{2} \rho_0 \delta v^2$ and magnetic $E_B = \frac{1}{2\mu_0} \delta B^2$ energies on $\langle |\epsilon_C| \rangle$, where δB and δv are respectively the fluctuating magnetic and flow velocity fields. First, one can see that for both types of turbulence, E_B/U (blue) dominates over E_K/U (red). However, the general trend of the compressible internal energy becomes comparable (or slightly larger) than the kinetic and magnetic energy with increasing $\langle |\epsilon_C| \rangle$ for magnetosonic cases. This trend is not seen on the Alfvénic cases indicating the prominent role of the internal energy in controlling the cascade rate. This last result contrasts significantly with the finding in the solar wind [10].

To study the anisotropic nature of the cascade rate for the different types of the MHD fluctuations, we examine the dependence of the estimated cascade rates on the mean angle Θ_{VB} between the local magnetic and flow

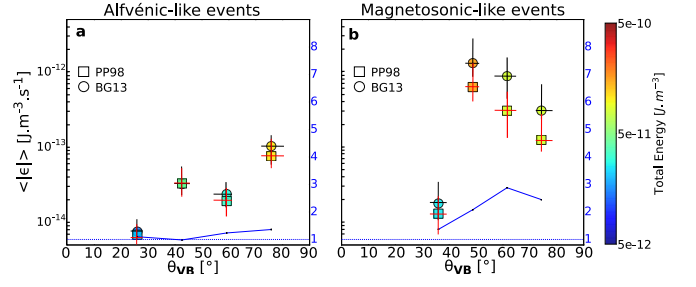


Figure 6: Compressible and incompressible energy cascade rates $\langle |\epsilon_C| \rangle$ and $\langle |\epsilon_I| \rangle$ as a function of the mean angle Θ_{VB} and the total energy (colored bar) for the Alfvénic (a) and magnetosonic (b) events. The blue line is the ratio $\mathcal{R} = \langle |\epsilon_C| \rangle / \langle |\epsilon_I| \rangle$.

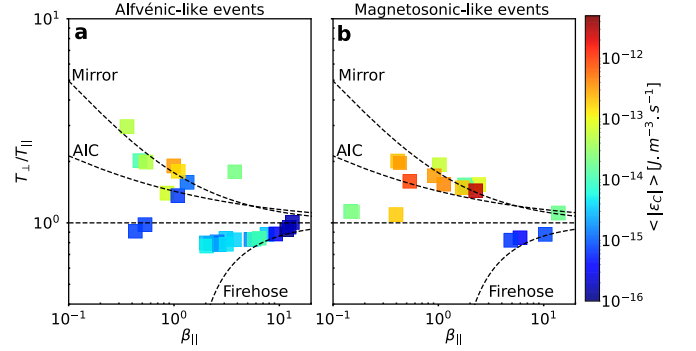


Figure 7: Compressible energy cascade rate $\langle |\epsilon_C| \rangle$ averaged into bins of proton temperature anisotropy (T_\perp/T_\parallel) vs β_\parallel for (a) the Alfvénic and (b) magnetosonic-like events. The dashed lines correspond to the mirror, the AIC, and firehose linear instabilities thresholds.

vectors. This approach has been already used in similar studies of solar wind turbulence [10, 47, 48]. Here we consider only the events for which Θ_{VB} is relatively stationary [10]. As one can see in Figure 6, for both models the cascade rate is lower in the parallel direction than in the perpendicular one. The same trend is observed for the total energy, except that for the magnetosonic events the highest cascade rate and total energy are observed at oblique angles $\Theta_{VB} \sim 50^\circ - 60^\circ$ (see discussion below). The second important observation is that the density fluctuations seem to reinforce the anisotropy of the cascade rate w.r.t. the Alfvénic turbulence: The ratio $\mathcal{R} = \langle |\epsilon_C| \rangle / \langle |\epsilon_I| \rangle$ (in blue) is close to 1 for the Alfvénic cases, but increases to ~ 3 for the magnetosonic ones at quasi-perpendicular angles. Numerical simulations of compressible MHD turbulence showed that fast magnetosonic turbulence is spatially isotropic while slow mode turbulence is anisotropic and has a spectrum $k_\perp^{-5/3}$ similarly to Alfvénic turbulence [13]. This first observation that density fluctuations enhance the anisotropy of the cascade rate suggests that a slow-like (or mirror) mode turbulence dominates the compressible fluctuations analyzed here [43, 49]. This result agrees with the analysis of the stability conditions of the plasma derived from the

linear Maxwell-Vlasov theory. Figure 7(a) shows that a large fraction of the Alfvénic-like cases that have the lowest values of the cascade rate correspond to a marginally stable plasma with $T_{\perp}/T_{\parallel} \sim 1$. This contrasts with the results from the magnetosonic turbulence (Figure 7(b)) showing that most of the events have strong temperature anisotropy and lie near the mirror instability threshold, where the energy cascade rate is the highest. Considering that the maximum growth rate of the linear mirror instability occurs at oblique angles $\Theta_{\mathbf{kB}}$ (approximated here by the angle $\Theta_{\mathbf{VB}}$) [50], the peak of the cascade rate and the total energy observed for $\Theta_{\mathbf{VB}} \sim 50^{\circ} - 60^{\circ}$ in Fig. 6 may be explained by energy injection into the background turbulent plasma through the mirror instability, which seems to enhance the dissipation rate. A similar relationship between incompressible cascade rate and kinetic plasma instabilities was found in the solar wind [51], however, deeper understanding of the connection between these two features of plasma turbulence requires further theoretical investigation [52]. Although the Taylor hypothesis (implicitly used in this work to interpret time lags τ as spatial increments) cannot generally be tested in single spacecraft data, the dominance of anisotropic slow (or mirror) like modes and the intrinsic anisotropic nature of the Alfvénic turbulence are arguments in favor of the validity of the Taylor hypothesis [53]. Indeed, k-filtering results (not shown here) obtained from four samples of Cluster data intervals to which the technique could be applied, support this conclusion (see, e.g., [49]).

Conclusions — The energy cascade rate in MHD turbulence in a the compressible magnetosheath plasma was found to be at least two orders of magnitude higher than in the (nearly) incompressible solar wind. Empirical laws relating the cascade rate to the turbulent Mach number were obtained. Density fluctuations were shown to amplify magnitude and the spatial anisotropy of the cascade rate in comparison with incompressible Alfvénic turbulence. This result and the analysis of the plasma stability conditions in the plane $(T_{\perp}/T_{\parallel}, \beta_{\parallel})$ indicate that the density fluctuations are carried by mirror (slow magnetosonic-like) mode driven by proton temperature anisotropy. These new fundamental features of compressible turbulence may have potential applications in the magnetosheath (e.g, turbulence-driven reconnection at the magnetopause [54, 55]) and in distant astrophysical plasmas. For instance, recently Zank *et al.* [15] showed the importance of the compressible magnetosonic modes in forming the turbulent energy cascade in the Local ISM, the Heliosheath (also a bounded region, by the termination shock and the Heliopause) using in-situ Voyager 1 data, results similar to the ones reported here.

Helpful discussions with N. Andres, S. Banerjee and H. Breuillard are gratefully acknowledged. The fields and the particles data of CLUSTER spacecraft come from the CAA (ESA) and of THEMIS B/C spacecraft from the AMDA science analysis system provided by the Centre de

Données de la Physique des Plasmas (IRAP, Université Paul Sabatier, Toulouse) supported by CNRS and CNES (CDPP, IRAP, France).

-
- [1] Zimbardo, Plasma Physics and Controlled Fusion, **48**, 128, (2006).
 - [2] A. A. Schekochihin, S. C. Cowley, W. Dorland, G. W. Hammett, G. G. Howes, E. Quataert, and T. Tatsuno, The Astrophysical Journal Supplement Series, **182**, 310, (2009)
 - [3] V. M. Papen, J. Saur, and O. Alexandrova, Journal of Geophysical Research: Space Physics, **119**, 4, (2014).
 - [4] C. Tao, F. Sahraoui, D. Fontaine, J. dePatoul, T. Chust, S. Kasahara, and A. Retino, Journal of Geophysical Research: Space Physics, **120**, 4, (2015).
 - [5] P. Song, C. T. Russell, and M. F., Journal of Geophysical Research: Space Physics, A6, **97**, 8295-8305, (1992).
 - [6] F. Sahraoui, J. L. Pinçon, G. Belmont, L. Rezeau, N. Cornilleau-Wehrlin, P. Robert, L. Mellul, J. M. Bosqued, A. Balogh, P. Canu, and G. Chanteur, J. Geophys. Res., **108**, 1335, (2003).
 - [7] E. A. Lucek, D. Constantinescu, M. L. Goldstein, J. Pickett, J. L. Pincon, F. Sahraoui, R. A. Treumann, and S. N. Walker, Space Science Reviews, **118**, (2005).
 - [8] V. Génot, E. Budnik, C. Jacquey, I. Dandouras and E. Lucek, Advances In Geosciences, (2009).
 - [9] G. G. Howes, S. D. Bale, K. G. Klein, C. H. K. Chen, C. S. Salem and J. M. TenBarge, The Astrophysical Journal Letters, **753**, 1, L19, (2012).
 - [10] L. Z. Hadid, F. Sahraoui, S. Galtier, The Astrophysical Journal, **838**, 1, 9, (2017).
 - [11] E. Vázquez-Semadeni, T. Passot and A. Pouquet, The Astrophysical Journal, **473**, 2, 881, (1996).
 - [12] Y. Lithwick and P. Goldreich, The Astrophysical Journal, **562**, 1, 279, (2001).
 - [13] J. Cho, and A. Lazarian, Phys. Rev. Lett., **88**, 245001, (2002).
 - [14] C. Federrath, J. Roman-Duval, R. S. Klessen, W. Schmidt, and M. M. Mac Low, AAP, **512**, A81, (2010).
 - [15] G. P. Zank, S. Du and P. Hunana, The Astrophysical Journal, **842**, 114, (2017).
 - [16] C.-Y. Tu, and E. Marsch, Space Sci. Rev., **73**, (1995).
 - [17] R. Bruno, and V. Carbone, Living Rev. Solar Phys., **2**, 4, (2005).
 - [18] F. Sahraoui, M. L. Goldstein, and P. Robert, and Y. V. Khotyaintsev, Phys. Rev. Lett., **102**, 23, 231102, (2009).
 - [19] H. Politano, and A. Pouquet, Phys. Rev. E, **57**, 21, (1998).
 - [20] C. W. Smith, K. Hamilton, B.J. Vasquez, and R. J. Leamon, Astrophys. J. Lett., **645**, L85 (2006).
 - [21] L. Sorriso-Valvo, R. Marino, V. Carbone, A. Noullez, F. Lepreti, P. Veltri, R. Bruno, B. Bavassano, and E. Pietropaolo, Phys. Rev. Lett., **99**, 115001, (2007)
 - [22] B. Vasquez, C. W. Smith, K. Hamilton, B. T. MacBride, and R. J. Leamon, J. Geophys. Res., **112**, 7101, (2007).
 - [23] B. MacBride, C. W. Smith, and M. A. Forman, Astrophys. J., **679**, 1644, (2008)
 - [24] J. E. Stawarz, C. W. Smith, J. Vasquez, M. A. Forman, and B. T. MacBride, Astrophys. J., **697**, 2, 1119, (2009).
 - [25] J. T. Coburn, C. W. Smith, B. J. Vasquez, J. E. Stawarz,

- and M. A. Forman, *Astrophys. J.*, **754**, 2, (2012)
- [26] Coburn, J. T., M. A. Forman, C. W. Smith, B. J. Vasquez, and J. E Stawarz, *Phil. Trans. R. Soc. A*, **373**, 20140150, (2015)
- [27] J. W. Freeman, *Geophysical Research Letters*, **15**, 1, 88-91, (1988).
- [28] E. Marsch, K. H. Muhlhauser, R. Schwenn, H. Rosenbauer, W. Pilipp, and F. M. Neubauer, *Journal of Geophysical Research: Space Physics*, **87**, A1, 52-72, (1982).
- [29] P. R. Gazis, *Journal of Geophysical Research: Space Physics*, **89**, A2, 775-785, (1984).
- [30] P. R. Gazis, *Journal of Geophysical Research: Space Physics*, **99**, A4, 6561-6573, (1994).
- [31] J. D. Richardson, K. I. Paularena, A. J. Lazarus, and J. W. Belcher, *Geophysical Research Letters*, **22**, 4, 325-328, (1995).
- [32] S. Banerjee, and S. Galtier, *Phys. Rev. E*, **87**, 013019, (2013).
- [33] S. Banerjee, L. Z. Hadid, F. Sahraoui, and S. Galtier, *The Astrophysical Journal Letters*, **829**, 2, L27, (2016).
- [34] C. P. Escoubet, R. Schmidt, and M. L. Goldstein, *Space Sci. Rev.*, **79**, 11-32, (1997).
- [35] V. Angelopoulos, *Space Science Reviews*, **141**, 1, 5, (2008).
- [36] A. Balogh, S. W. H. Cowley, M. W. Dunlop, D. J. Southwood, J. G. Thomlinson, K. H. Glassmeier, G. Musmann, H. Luehr, M. H. Acuna, D. H. Fairfield, Cluster: Mission, Payload, and Supporting Activities, (1993).
- [37] H. Reme, J. M. Bosqued, J. A. Sauvaud, A. Cros, J. Dandouras, C. Austin, J. Bouyssou, Th. Camus, J. Cuvido, C. Martz, J. L. Medale, H. Perrier, D. Romefort, J. Rouzaud, C. D' Uston, E. Mobius, K. Crocker, M. Granoff, L. M. Kistler, M. Popecki, D. Hovestadt, B. Klecker, G. Paschmann, M. Scholer, C. W. Carlson, D. W. Curtis, R. P. Lin, J. P. Mcfadden, V. Formisano, E. Amata, M. B. Bavassano-CATTANEO, P. Baldetti, G. Belluci, R. Bruno, G. Chionchio, A. Di Lellis, E. G. Shelley, A. G. Ghielmetti, W. Lennartsson, A. Korth, H. Rosenbauer, R. Lundin, S. Olsen, G. K. Parks, M. McCarthy, and H. Balsiger, *Space Science Reviews*, **79**, 1, 303-350, (1997).
- [38] A. D. Johnstone, C. Alsop, S. Burge, P. J. Carter, A. J. Coates, A. J. Coker, A. N. Fazakerley, M. Grande, R. A. Gowen, C. Gurgiolo, B. K. Hancock, B. Narheim, A. Preece, P. H. Sheather, J. D. Winningham, R. D. and Woodliffe, **79**, 1, 351-398, (1997).
- [39] J. G. Trotignon, P. M. E. Décréau, J. L. Rauch, E. Le Guirriec, P. Canu, and F. Darrouzet, *Cosmic Research*, **41**, 4, 345-348, (2003).
- [40] H. U. Auster, K. H. Glassmeier, W. Magnes, O. Aydogar, W. Baumjohann, D. Constantinescu, D. Fischer, K. H. Fornacon, E. Georgescu, P. Harvey, O. Hillenmaier, R. Kroth, M. Ludlam, Y. Narita, R. Nakamura, K. Okrafka, F. Plaschke, I. Richter, H. Schwarzl, B. and Stoll, A. Valavanoglou, and M. Wiedemann, New York, NY: Springer New York, (2009).
- [41] McFadden, J. P., Carlson, C. W., Larson, et al. 2009, pp. 277-302. New York, NY: Springer New York.
- [42] S. Y. Huang and L. Z. Hadid and F. Sahraoui and Z. G. Yuan and X. H. Deng, *The Astrophysical Journal Letters*, **836**, 1, L10, (2017).
- [43] L. Z. Hadid, F. Sahraoui, K. H. Kiyani, A. Retino, R. Modolo, P. Canu, A. Masters and M. K. Dougherty, *The Astrophysical Journal Letters*, **813**, 2, L29, (2015).
- [44] S. P. Gary, and C. W. Smith, *J. Geophys. Res.*, **114**, A12105, (2009)
- [45] F. Sahraoui, G. Belmont, and M. L. Goldstein, *Astrophys. J.*, **748**, 100, (2012).
- [46] C. S. Salem, G. G. Howes, D. Sundkvist, S. D. Bale, C. C. Chaston, C. H. K. Chen, and F. S. Mozer, *ApJ Lett.*, **745**, L9, (2012).
- [47] R. Marino, L. Sorriso-Valvo, R. D'Amicis, V. Carbone, R. Bruno, P. Veltri, *Astrophys. J.*, **750**, (2012)
- [48] C. W. Smith, and J. E. Stawarz, and B. J. Vasquez, and M. A. Forman, and B. T. MacBride, *Phys. Rev. Lett.*, **103**, 201101, (2009)
- [49] F. Sahraoui, G. Belmont, L. Rezeau, and N. Cornilleau-Wehrlin, and J. L. Pincon, and A. Balogh, *Phys. Rev. Lett.*, **96**, 075002, (2006).
- [50] O. A. Pokhotelov, O. G. Onishchenko, R. Z. Sagdeev, M. A. Balikhin, and L. Stenflo, *Journal of Geophysical Research: Space Physics*, **109**, A3, (2004).
- [51] K. T. Osman, W. H. Matthaeus, K. H. Kiyani, B. Hnat, and S. C. Chapman, *Phys. Rev. Lett.*, **111**, 201101, (2013).
- [52] M. W. Kunz, A. A. Schekochihin, and J. M. Stone, *Phys. Rev. Lett.*, **112**, 205003, (2014).
- [53] G. G. Howes and K. G. Klein and J. M. TenBarge, *The Astrophysical Journal*, **789**, 2, 106, (2014).
- [54] G. Belmont and L. Rezeau, *J. Geophys. Res.*, **106**, (2001).
- [55] H. Karimabadi, and V. Roytershteyn, and H. X. Vu, and Y. A. Omelchenko, and J. Scudder, and W. Daughton, and A. Dimmock, and K. Nykyri, and M. Wan, and D. Sibeck, and M. Tatineni, and A. Majumdar, and B. Loring, and B. Geveci, *Physics of Plasmas*, **21**, 6, (2014).